IL NUOVO CIMENTO Vol. 26 C, N. 1 Gennaio-Febbraio 2003

Water vapour absorption effects on solar radiation in an Apennine valley from hygrometric measurements of precipitable water taken at various altitudes(*)

C. Tomasi, A. Lupi, S. Marani and V. Vitale

Institute of Atmospheric Sciences and Climate (ISAC), CNR
Via Gobetti 101, I-40129 Bologna, Italy

(ricevuto il 27 Marzo 2002; approvato il 18 Luglio 2002)

Summary. — Hygrometric ratio measurements were simultaneously taken on six autumn clear-sky days of 1981 and 1982 by employing four Volz sun-photometers and the FISBAT sun-photometer at five stations located at different altitudes along the western slope of the Leo Valley, in the Apennines (Italy). Due to the solar heating of ground, intense upslope breezes forming during the early morning caused the vertical transport of more humid air from the bottom of the valley toward the ridge of the mountain chain. Precise calibration curves of the hygrometric ratio were defined on the basis of criteria suggested by the atmospheric infrared hygrometry technique and using the calibration constants found through an accurate intercomparison procedure. Examining the sun-photometric measurements by means of these calibration curves, precipitable water was determined at all stations, with the frequency of one measurement every 15 minutes from the early morning to one hour after noon. Daily homogeneous time-patterns of precipitable water were defined at the various stations, showing that this quantity varies appreciably during the morning at all stations, sometimes presenting daily increases of more than 40% at the lower stations. Average values of absolute humidity were then determined within the four atmospheric layers defined by the station altitudes, finding that the convective transport of humid air along the valley slopes can produce important variations within the atmospheric layer below the 1.6 km height.

(*) The authors of this paper have agreed to not receive the proofs for correction.

For these moisture conditions of the atmosphere, calculations of the time-variations caused by water vapour absorption in the downwelling flux Φ_1 of global solar radiation reaching the ground were made at the various stations, as well as of those in the upwelling flux Φ of solar radiation at the top-level of the atmosphere. The results indicate that: i) flux Φ_1 can appreciably decrease due to water vapour absorption, by 10 to 20 W m^{-2} at the highest station of Mt. Cimone and by 70 to 80 W m^{-2} at the lowest station situated on the bottom of the Leo Valley, and ii) the changes caused by water vapour absorption in the upwelling flux Φ were estimated to range usually between about 5 W m^{-2} at the Mt. Cimone station and more than 25 W m^{-2} at the lowest station. In particular, as a consequence of the time-variations in both precipitable water and solar elevation angle, the change $\Delta\Phi$ caused by water vapour in the instantaneous outgoing flux of solar radiation at noon was found to increase almost linearly as a function of precipitable water throughout the range from 0.8 to 1.8 g cm^{-2}, with an average slope coefficient equal to 12.5 W m^{-2} per unit variation of precipitable water.

PACS 42.68.-w – Atmospheric optics.
PACS 92.60.-e – Meteorology.
PACS 92.60.Jq – Water in the atmosphere (humidity, clouds, evaporation, precipitation).
PACS 92.60.Vb – Solar radiation.
PACS 92.60.Ry – Climatology.

1. – Introduction

Because of the intense radiative cooling occurring during the nocturnal hours of autumn clear-sky days, strong thermal inversions form in the Po Valley area and in the lateral valleys ascending the northern slope of the Apennine chain, presenting the most marked stability conditions a short time before sunrise. During the morning, for cloudless conditions of the sky, the solar radiation usually heats the ground so strongly as to cause gradually more intense convective motions [1]. The result is that, within less than one hour after sunrise, moderate upslope anabatic winds begin to move along the gently-sloping sides of the Apennine valleys, and the air relative humidity of air changes considerably within the lower atmospheric layers. Thus, the columnar atmospheric content of water vapour (commonly called precipitable water) tends very often to gradually increase, until reaching the highest values towards the noon, mainly due to the transport of more humid air from the Po Valley and the lower part of the Apennine valley towards the head of the valley. Because of the variations in precipitable water, which are particularly marked at the lower stations of the valley, the incoming solar radiation is found to be absorbed by water vapour to an extent that varies according to the different heights. Thus, the solar radiation balance at the ground is expected to vary considerably at all altitudes.

To give a measure of such variations in the incoming flux of solar radiation, we performed some calculations of the downwelling flux of global solar radiation using the 6S computer code [2] for relative optical air mass values equal to 1, 2, 3 and 5 (corresponding to values of the apparent zenith angle θ of the Sun approximately equal to 0°, 60°, 71° and 79°, respectively) and for the "U. S. Standard Atmosphere, 1976" model [3], where i) precipitable water is equal to 1.42 g cm^{-2}, ii) aerosol particles are represented in terms

TABLE I. – *Measurement stations where the multispectral sun-photometers were employed during the two field campaigns of* 1981 *and* 1982.

Station	Year 1981			Year 1982		
	Site	Height (m a.m.s.l.)	Sun-photometer	Site	Height (m a.m.s.l.)	Sun-photometer
A	Le Chiuse	505	Volz No. 587	Le Chiuse	505	Volz No. 587 and 595
B	Le Ville	726	Volz No. 591	La Tintoria	826	Volz No. 591
C	Sestola (Piscina)	970	Volz No. 477	Sestola (Ville)	1118	Volz No. 596
D	Pian del Falco	1320	Volz No. 590	Mt. Calvanella	1528	Volz No. 590
E	–	–	–	Mt. Cimone	2165	FISBAT (example E)

of a continental particle polydispersion yielding a visual range of 23 km at ground-level, and iii) the surface albedo characteristics are assumed to be those of a green vegetation cover. The results indicate that the global solar radiation reaching the ground is equal to about 82% , 36% , 21% and 10% of the solar constant (equal to 1367 W m^{-2} [4]) for $\theta = 0°$, $60°$, $71°$ and $79°$, respectively, these changes being mainly produced by the increase in the water vapour mass and aerosol particulate mass distributed along the sun path.

To give evidence of the important absorption of solar radiation by water vapour, we also assumed gradually increasing values of precipitable water in the above atmospheric model, from 0 to 1.42 g cm^{-2} in steps of 0.1 g cm^{-2}, finding that the presence of a water vapour mass of 1.42 g cm^{-2} in the vertical atmospheric column causes a relative decrease in the downwelling flux of global solar radiation equivalent to about 11%, 14%, 16% and 20% for $\theta = 0°$, $60°$, $71°$ and $79°$, respectively. This means that even a small variation of 0.1 g cm^{-2} in precipitable water causes a percentage variation in the global solar radiation flux reaching the ground along various slant sun-paths, ranging between 0.8% and 1.4% as the solar zenith angle increases from $0°$ to $79°$, which correspond to variations in the solar radiation flux absorbed by water vapour equal, on the average, to 9.7 W m^{-2} at $\theta = 0°$, 5.7 W m^{-2} at $\theta = 60°$, 4.0 W m^{-2} at $\theta = 71°$ and 2.5 W m^{-2} at $\theta = 79°$. Considering that the solar elevation angle is close to $60°$ around the noon on the last days of October, these calculations confirm that the radiative effects produced by a precipitable water change of 0.1 g cm^{-2} can be of comparable magnitude to those induced by marine aerosol particles at the top of the atmosphere in remote oceanic areas, where the aerosol optical depth at visible wavelengths ranges between 0.05 and 0.1 [5,6].

Taking the findings into account, we decided to re-examine the large set of direct solar irradiance measurements carried out by our group [7] on clear-sky autumn days in 1981 and 1982. These old measurements were performed using various multi-wavelength sun-photometers positioned at five stations situated at different heights along the western slope of the Leo Valley in the Apennines, about 50 km south-west of Bologna (Italy). Four

Volz sun-photometers, model A [8], were used during the field campaign of 1981 at four stations positioned at altitudes varying from 505 to 1320 m a.m.s.l., as shown in table I. Direct solar irradiance measurements were regularly taken every 15 minutes at the four wavelengths equal to 380, 500, 875 (or 886) and 946 nm, the third wavelength being centred within a very transparent window of the near-infrared atmospheric transmission spectrum and the fourth in the middle of the strong absorption band of water vapour called $\rho\sigma\tau$ [9]. Simultaneous measurements were taken at the top-level station of Mt. Cimone (2165 m a.m.s.l.) with the AM sun-photometer of the Meteorological Service of the Italian Air Force, equipped only with two passband interference filters with peak transmission wavelengths of 380 and 500 nm [10] and, hence, not suitable for precipitable water measurements.

During the second field campaign in autumn 1982, we used the Volz (model A) sun-photometers listed in table I at other stations located at altitudes varying from 505 to 1528 m a.m.s.l., while more sophisticated sun-photometric measurements were performed at the Mt.Cimone (2165 m a.m.s.l.) station with the frequency of one spectral scanning per hour, employing the eight-wavelength FISBAT sun-photometer (example E) to provide hygrometric ratio measurements and precipitable water evaluations [11]. On all the measurement days of both campaigns, regular and continuous measurements of air pressure, temperature and relative humidity were recorded by the Meteorological Service of the Italian Air Force at the Sestola (1030 m a.m.s.l.) and Mt. Cimone (2165 m a.m.s.l.) stations by means of both barographs and thermohygrographs. The time-patterns of air temperature and relative humidity recorded at both stations on two measurement days are shown in fig. 1.

The procedure followed to analyse the sun-photometric measurements taken with the Volz and FISBAT instruments to determine the precipitable water time-patterns at the various stations is described in the following sections, together with the main results. The time-patterns were subsequently examined to determine the time-variations in the vertical distribution features of absolute humidity and represent the mean moisture features of the atmospheric ground layer taking place in a valley where an upslope wind circulation regime is present.

2. – The atmospheric hygrometry technique at near-infrared wavelengths

The atmospheric hygrometry technique at near-infrared wavelengths is based on the comparison of simultaneous ground-based measurements of direct solar irradiance performed using a spectrophotometer or a sun-radiometer equipped with two narrow band-pass interference filters: one of the filters has peak-transmission wavelength λ_b chosen within the central part of a near-infrared water vapour absorption band (like the above-mentioned $\rho\sigma\tau$ band covering the spectral range from 0.89 to 1.00 μm wavelength [9]), while the other filter has peak-transmission wavelength λ_w centred in the middle of a nearby window. The first filter is used to achieve a strong absorption measurement of atmospheric water vapour, while the latter serves to obtain a reference measurement of direct solar irradiance within a spectral interval characterised by very weak features produced by water vapour absorption. Due to the large difference in the strength of the water vapour absorption effects occurring within the two narrow spectral intervals, the hygrometric ratio R between the two output voltages $J(\lambda_b)$ and $J(\lambda_w)$ given by the sun-photometer turns out to be closely related to the water vapour mass distributed along the sun path. Therefore, precise measurements of precipitable water (defined as the water vapour mass in the vertical atmospheric column of unit cross section and usu-

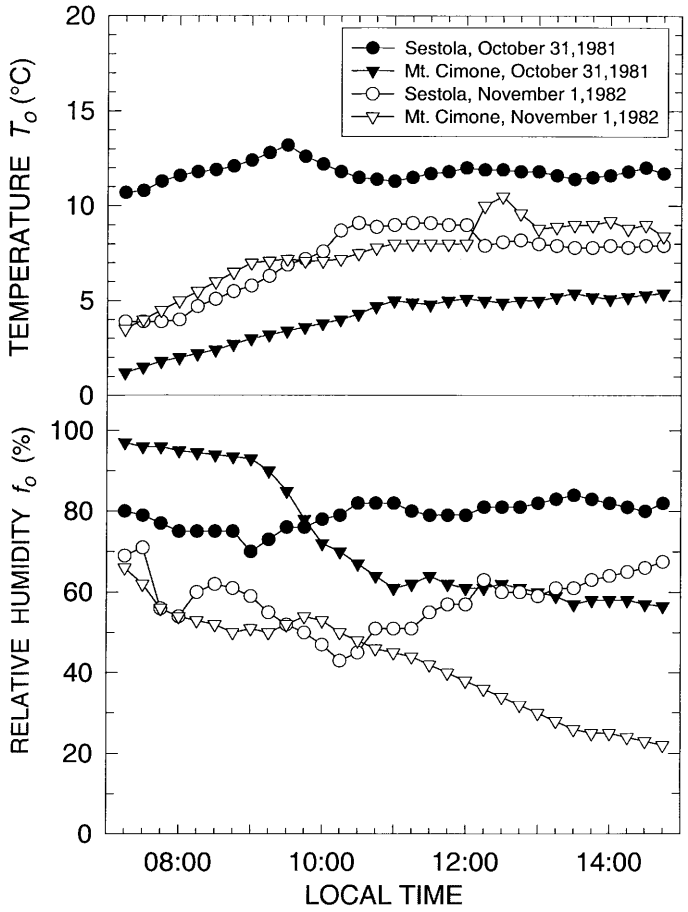

Fig. 1. – Time-patterns of air temperature T_0 and relative humidity f_0 routinely measured at the Sestola (970 m a.m.s.l.) (circles) and Mt. Cimone (2165 m a.m.s.l.) (triangles) stations during the morning periods of October 31, 1981 (solid symbols) and November 1, 1982 (open symbols).

ally measured in g cm^{-2} or cm STP) can be determined from the measurements of ratio $R = J(\lambda_b)/J(\lambda_w)$, only if realistic and accurate measurements of the optical length of the sun-path are available, for instance by means of the correct use of the relative optical mass function for water vapour, which can be evaluated with good precision from the apparent solar elevation angle observed during the measurements [12].

Taking spectrophotometric measurements of incoming solar radiation, Fowle [13, 14] was the first to show that a close relationship exists between the atmospheric transmission characteristics observed in the near-infrared spectrum and the water vapour amount present in the atmospheric vertical column. Further investigations on the spectral features of the infrared absorption bands of atmospheric water vapour were performed by several others [15-18] who proposed various instruments and analytical methods for measuring the water vapour mass present along the sun-path. Examining the solar spectrum features and considering that the predominant radiative effects caused by water vapour

absorption can be described with good approximation by the random statistical model of a strong absorption band proposed by Goody [19], Gates and Harrop [20] found that the natural logarithm of hygrometric ratio R is linearly related to the square-root of precipitable water, in agreement with the approximated form of the Goody [19] band model for strong absorbers. The reliability of this simple analytical form was clearly confirmed by direct solar irradiance measurements taken for different precipitable water values and solar elevation angles in the 1.08–1.26 μm wavelength range totally including the water vapour band indicated by the Greek letter Φ [21].

Two years later, the square-root dependence law was applied to field measurements taken with sun-photometers equipped with two interference filters peaked at about 0.94 μm and 0.88 μm wavelengths [8, 22], defining reliable procedures for determining precipitable water from simultaneous measurements of direct solar radiation. Examining direct solar irradiance measurements taken with a seven-channel solar radiometer and analysing the measurements performed with two bandpass interference filters centred at the 0.873 μm and 0.942 μm wavelengths, Pitts *et al.* [23] found a value of the exponent of the total water vapour mass along the sun-path to be equal to 0.562, instead of 0.5, as previously established by others through various field measurements [8, 11, 20, 22]. However, the results found by Pitts *et al.* [23] only apparently contradicted the square-root dependence law and the use of a water vapour mass exponent equal to 0.5 for giving form to the dependence function of hygrometric ratio on the atmospheric water vapour mass distributed along the sun-path. In fact, further studies demonstrated that this exponent could vary between about 0.83 and 0.04 without causing a statistically significant change in the empirical fit of the hygrometric ratio logarithm plotted versus the power of precipitable water [24]. In examining multispectral sets of sun-photometric measurements of direct solar irradiance, carried out at the Terra Nova Bay station in Antarctica during January and February 1988 and 1989, Tomasi *et al.* [25] adopted a specially developed infrared hygrometry technique. It was based on the simultaneous use of the direct solar radiation measurements performed within three wavelength intervals centred at 865.2 nm (first window), 939.0 nm (water vapour band) and 1047.4 nm (second window), so as to compensate for and minimize the dispersion effects due to the spectral variability of both aerosol extinction and Rayleigh scattering. Both these attenuation effects are produced with intensities decreasing with wavelength at the three above-mentioned wavelengths by percentages, increasing appreciably in cases where the two window-wavelengths are far enough from that positioned in the middle of the water vapour band. A more sophisticated procedure was then proposed by Thome *et al.* [26,27] based on the combined use of three-channel and two-channel methods for analysing the solar radiation measurements with a modified Langley technique. In this procedure, the water vapour optical depth was determined and subsequently converted to total precipitable water by employing a very careful transmission model for the 0.94 μm water vapour band, and following an efficient method for minimising the aerosol extinction effects which can appreciably alter the water vapour absorption measurements. This was done by evaluating the aerosol optical depth at 0.94 μm wavelength from the simultaneous direct solar irradiance measurements taken within the two window-channels, simultaneously using atmospheric transmission models for Rayleigh scattering defined within the three radiometric channels, in order to reduce the variable errors associated with the above-mentioned extinction processes until rendering them completely negligible.

Precise measurements of precipitable water were performed by our group during the CLEARCOLUMN (ACE-2) experiment, using two examples of the multispectral sun-photometer, model ASP (Antarctic Sun Photometer) at the Sagres (50 m a.m.s.l.) and

Mt. Foia (920 m a.m.s.l.) stations in the southern Portugal, during June and July 1997 [28]. By means of calibration curves based on the rigorous application of the square-root dependence curve of hygrometric ratio on the water vapour mass present along the sun-path, we found that the estimates of precipitable water obtained at Sagres from the measurements of the pair of hygrometric ratios $R = J(947.7\text{ nm})/J(861.2\text{ nm})$ and $R = J(947.7\text{ nm})/J(1025.7\text{ nm})$ differed very little one from the other, on all the measurement days and at the different hours of the same day, showing that the discrepancies between the aerosol extinction effects within each of the two window-channels and the water vapour band channel can cause in reality only very small errors, provided that the window-channels are relatively narrow and their peak-wavelengths are chosen not too far from that of the band-channel. The above errors were estimated to be lower than a few percents in all cases where the solar zenith angle θ was smaller than 80° (*i.e.* for relative optical air mass smaller than 5.5) and the band- and window-channel measurements were performed within a few seconds only [28], thus obtaining the triplet of sun-photometric output voltages $J(861.2\text{ nm})$, $J(947.7\text{ nm})$ and $J(1025.7\text{ nm})$ for very close values of the relative optical mass for water vapour [29].

On the basis of the above remarks and results, the Volz and FISBAT sun-photometer measurements of the hygrometric ratio R performed during the two campaigns of autumn 1981 and 1982 were considered to be suitable for providing homogeneous evaluations of precipitable water. With this aim, we decided to prepare a reliable set of calibration curves capable of accurately describing the dependence features of R on the water vapour mass present along the sun-path, which could be reliably used for the six Volz sun-photometers employed during the two campaigns. This was achieved through an accurate intercomparison procedure enabling us to define homogeneous calibration curves for all the said instruments.

3. – Calibration of the hygrometric ratio

As pointed out above, the calibration curve of hygrometric ratio R is usually determined as the best-fit curve of a data-set obtained by plotting the hygrometric ratio measurements (all normalised to standard air pressure conditions at the ground) as a function of the square root of the product of precipitable water w by the relative optical mass m for water vapour. Parameter m provides the measure of the ratio between i) the optical mass of the water vapour distributed along the oblique trajectory described by the solar rays passing through the atmosphere, this quantity actually causing the absorption of the incoming solar radiation, and ii) the optical water vapour mass along the vertical atmospheric path [4, 12, 29]. Thus, according to the above-mentioned procedures [8, 11, 20-22], we considered the following points:

1) The ratio between the transmission terms relative to Rayleigh scattering [30] at the two wavelengths λ_b and λ_w follows a well-defined dependence curve on the relative optical air mass and, hence, on the relative optical mass m for water vapour, since the difference between the Rayleigh optical depths at the two wavelengths λ_b and λ_w assumed stable values on all the measurement days for similar values of the total air pressure at ground-level. In fact, Rayleigh scattering optical depth is approximately proportional to the product of the inverse of the fourth power of wavelength by the ground-level air pressure. Thus, the ratio between the two Rayleigh scattering optical depths does not depend in practice on the air pressure conditions at the station level and is nearly proportional to the fourth power of ratio λ_b/λ_w.

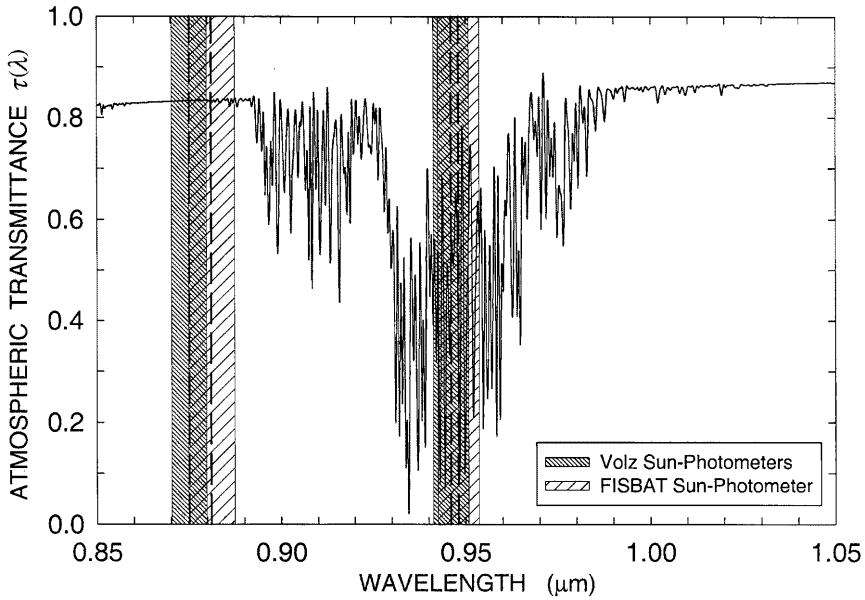

Fig. 2. – Spectral curve of atmospheric transmittance $\tau(\lambda)$ in the 0.85–1.05 μm wavelength range, as calculated for a spectral resolution of 0.44 nm at wavelength $\lambda = 0.94$ μm using the MODTRAN 3.7 code [32] for the "U. S. Standard Atmosphere, 1976" model [3] presenting a 23 km visual range at sea-level and the rural aerosol extinction model [31]. The vertical dashed lines indicate the peak-wavelengths of the pairs of interference filters mounted for hygrometric use on five of the six Volz sun-photometers used during the two campaigns and the FISBAT sun-photometer (example E), while the vertical shaded bands define the spectral positions of the half-bandwidths of the same passband interference filters.

2) The aerosol transmission terms relative to the aerosol particle attenuation exhibit only small differences at the two wavelengths λ_b and λ_w in all cases where the aerosol optical depth in the near-infrared spectral range is relatively low, and the corresponding values of the relative optical air mass were taken within a very short time-interval of a few seconds [31]. Since these conditions were satisfied on all the measurement days of the 1981 and 1982 campaigns, we estimated that the ratio between the aerosol transmission terms at wavelengths λ_b and λ_w assumed values differing from the unity by less than $\pm 5\%$ in the presence of atmospheric transparency conditions like those observed on the six measurement days.

On the basis of these remarks, we considered that i) the ratio between the two Rayleigh transmission terms follows a close dependence form on the relative optical mass m, and ii) the ratio between the two aerosol transmission terms is close to the unity for all the measurement conditions. Thus, the time-variations in the hygrometric ratio $R = J(\lambda_b)/J(\lambda_w)$ due to spectral differences in both Rayleigh scattering and aerosol optical depths are expected to be so limited on all the measurement days as to cause only a slight scatter of data. Consequently, the time-changes in the hygrometric ratio R are mainly due to the time-variations in the relative optical mass m and precipitable water w. Therefore, the values of R given by the Volz and FISBAT sun-photometers were assumed to be proportional through a constant factor R_0 to the ratio between i) the water vapour transmission function within the middle part of the $\rho\sigma\tau$ band (which can be correctly

represented in terms of the square-root dependence form defined by Goody [19]), and ii) the water vapour transmission function typical of a very transparent window of the solar spectrum, like that appearing with its central part at about 0.86 μm wavelength in fig. 2, on the left of the $\rho\sigma\tau$ water vapour band. As is well established in the literature [4,8,9,11,19-22], the monochromatic transmission function within the main windows of the solar spectrum, like that centred at 0.86 μm wavelength, can all be realistically represented in terms of a weak absorption model following an approximately linear dependence form on the water vapour mass. The spectral absorption characteristics of the $\rho\sigma\tau$ band and the spectral transmittance features of the two nearby atmospheric windows are shown in fig. 2, with a spectral resolution better than 0.5 nm. The wavelength intervals covered by the band- and window-channels defined by the narrow passband interference filters mounted on the Volz and FISBAT sun-photometers are also shown in fig. 2, to give evidence of the marked differences characterising the water vapour absorption features within the various channels.

Therefore, we represented the dependence curve of the hygrometric ratio R on the total water vapour mass present along the sun-path (given by the product of precipitable water w by the relative optical mass m) using the following square-root approximation form:

$$R = R_0 \exp[-K(mwp_0/1013.25)^{1/2}] , \tag{1}$$

where the Rayleigh scattering and aerosol extinction terms do not appear in an explicit form. In eq. (1):

– factor R_0 closely depends not only on the spectral features of the extra-terrestrial solar irradiance, but also on the spectral responsivity characteristics of the sun-photometer within the two spectral channels employed in the atmospheric hygrometry technique;
– parameter K is closely related to the spectral strength of the absorption features presented by the $\rho\sigma\tau$ water vapour band within the water vapour channel with peak-wavelength λ_b, and to a lesser extent depends on the spectral features of weak absorption produced by water vapour within the selected window-channel;
– m is the relative optical mass for water vapour, calculated according to the Kasten [29] formula and the correction factors proposed by Tomasi *et al.* [12] for the U. S. Standard Atmosphere 1976 model [3], and
– p_0 is the total air pressure measured in hPa at the station level.

The values of intercept R_0 and slope coefficient K in eq. (1) can be determined for each set of hygrometric measurements providing pairs of values of ratio R and slant-path water mass $m\,w$, by i) plotting the natural logarithms of R as a function of the square root of the product $m\,w$, normalised to standard air pressure conditions at the ground, and ii) drawing the least-square line to define both the intercept R_0 at $m = 0$ and the slope coefficient K. However, when the field measurements are analysed to define the best-fit curve in terms of eq. (1), the determination of the slope coefficient K and intercept R_0 is influenced by the dispersion errors due to the variability of aerosol extinction, as well as the systematic errors caused by neglecting the Rayleigh scattering transmission terms, since both such errors vary considerably as a function of parameter m. However, when an empirical calibration curve has been determined in the simple form of eq. (1), precipitable water w can be evaluated from each measurement of hygrometric ratio R taken at relative optical mass m, by using the following inverse formula derived from

eq. (1):

$$w = \frac{1013.25\ \ln^2 (R_0/R)}{K^2\ m\ p_0}\,. \tag{2}$$

In order to determine homogeneous sets of the calibration constants R_0 and K for their correct use in eq. (2), in all cases where this algorithm is applied to the various sun-photometric measurements, we decided to carry out a series of intercomparison measurements simultaneously taken with the six Volz sun-photometers listed in table I and the FISBAT (example E) sun-photometer. The intercomparison campaigns were performed at the following sites:

a) Poggioraso (906 m a.m.s.l.), a few kilometres from Sestola, from October 24 to 31, 1981;

b) Passo delle Radici (1529 m a.m.s.l.) in the Apennines, about 20 km west of Sestola, from November 10 to 18, 1981;

c) Bologna (35 m a.m.s.l.) on numerous clear-sky days from February to June 1981;

d) Molinella in the Po Valley, about 28 km north-east of Bologna, on several clear-sky days from February to July 1982;

e) Poggioraso (906 m a.m.s.l.) in November 1982.

We collected large sets of simultaneous measurements of ratio R, as obtained from the output voltages $J(\lambda_b)$ and $J(\lambda_w)$ supplied by the various sun-photometers, together with:

i) the simultaneous measurements of air pressure p_0 at the station level;

ii) the measurements of the internal temperature of the Volz sun-photometers, for which the output voltages $J(\lambda_b)$ and $J(\lambda_w)$ were corrected following the procedure suggested by the manufacturer to remove the voltage drift effects due to the internal temperature variations (and, hence, obtaining sun-photometric output voltages all normalised to the mean temperature of 20 °C [8]); and

iii) the records of the measurement-times of both output voltages $J(\lambda_b)$ and $J(\lambda_w)$ read with the precision of a few seconds.

For these precise measurement times, we calculated the astronomic coordinates of the Sun and the corresponding apparent solar elevation angle h [4], taking into account the longitude and latitude coordinates of each station and using appropriate algorithms for determining the atmospheric refraction effects occurring during the measurement periods for standard atmospheric conditions [33]. The purpose was to obtain precise values of the relative optical mass m at all the measurement times by calculating them as a function of h, according to the dependence function and the correction factors defined for standard conditions of the mid-latitude atmosphere [12, 29].

For each pair of values of R and m, we first attempted to determine the values of precipitable water w using in eq. (2) the original values of the calibration constants R_0 and K proposed by the manufacturer [8] and given in table II. However, the results of this preliminary approach were judged to be unconvincing, since large discrepancies were found among the estimates of w provided simultaneously by the various Volz sun-photometers, like those shown by the time-patterns of w in the left part of fig. 3, determined from the measurements taken at Bologna on February 27, 1982. These time-patterns clearly exhibit discrepancies of more than 35%, as can be seen for instance from a comparison of the time-patterns of w given by sun-photometer No. 591 with those of sun-photometer No. 595. We therefore decided to re-calibrate the hygrometric ratios R given by the six

TABLE II. – *Values of peak-wavelengths λ_b (water vapour band) and λ_w (window) of the interference filters mounted on the seven sun-photometers to perform measurements of the hygrometric ratio R. The fourth and fifth columns show the best-fit values of the calibration constants R_0 and K suitable for use in eq.* (1) *to calculate precipitable water w, which are compared with those proposed by the manufacturer (in brackets). The sixth column provides the corresponding regression coefficients found for the present experimental data-sets.*

Sun-photometer example	Wavelength λ_b (nm)	Wavelength λ_w (nm)	Intercept R_0	Slope coefficient K (g $^{-0.5}$ cm)	Regression coefficient r
Volz No. 477	946	875	1.7390 (1.66)	0.6823 (0.5756)	−0.989
Volz No. 587	946	886	2.1130 (2.22)	0.7384 (0.4799)	−0.998
Volz No. 590	946	875	1.9721 (1.915)	0.7426 (0.7281)	−0.996
Volz No. 591	946	875	1.8948 (2.02)	0.7122 (0.7281)	−0.997
Volz No. 595	946	875	2.2303 (2.08)	0.7720 (0.7281)	−0.999
Volz No. 596	946	875	2.0706 (2.06)	0.6943 (0.7281)	−0.998
FISBAT (example E)	948.0	881.1	7.0234	0.7764	−0.993

Volz sun-photometers, determining the new values of constants R_0 and K in eq. (2) and checking the reliability of the original calibration constants determined for the FISBAT (example E) sun-photometer [11], which are also given in table II. With this aim, for all the intercomparison data-sets collected at Bologna and Molinella, we associated each ratio R measured with one of the six Volz sun-photometers with a value of w calculated by averaging the following values:

1) the mean value obtained from the set of simultaneous estimates of w found using the original values of the calibration constants R_0 and K to analyse the measurements given by the six Volz sun-photometers [8], and

2) the simultaneous value of w calculated from the radiosounding measurements performed at 12:00 GMT at the San Pietro Capofiume station (9 m a.m.s.l.), situated in the middle of the Po Valley, 25 km north-east of Bologna and 2 km north-west of Molinella, taking also into account the ground-level absolute humidity measurements performed on that day at the stations of Bologna and Molinella.

More precisely, each value of w considered above at point 2) was estimated as equal to the product of the following three quantities: i) the daily value of w calculated from the absolute humidity vertical profile defined from the radiosounding data within the atmospheric altitude range from the station level to the highest level reached by the radiosonde, ii) the ground-level value of absolute humidity simultaneously measured at the station of Bologna or Molinella, and iii) the inverse of the ground-level absolute humidity value measured by the radiosonde at 12:00 GMT at San Pietro Capofiume.

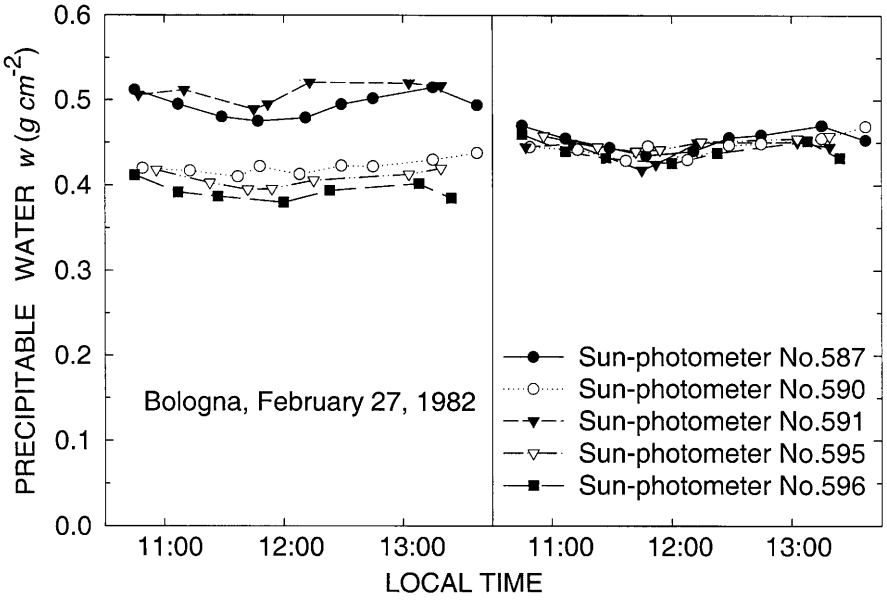

Fig. 3. – Comparison between the time-patterns of precipitable water w determined from the measurements of hygrometric ratio R taken with five Volz sun-photometers at Bologna (35 m a.m.s.l.) on February 27, 1982, using different pairs of calibration constants R_0 and K in eq. (1): those shown on the left were obtained using the original values of R_0 and K given by the manufacturer [8], while those on the right were determined using the new values of R_0 and K obtained following the present intercomparison procedure.

Moreover, since the stations of Poggioraso and Passo delle Radici are both rather far from the radiosounding station, we assumed for all the intercomparison measurements carried out at the two mountain stations that the true value of w suitable for use in the calibration procedure of the hygrometric ratios provided by the six Volz sun-photometers is the value obtained at each measurement time by averaging i) the mean value calculated from the estimates of w provided by the six Volz sun-photometers [8] using the original values of the calibration constants R_0 and K, and ii) the value of w obtained from the simultaneous measurement of hygrometric ratio taken with the FISBAT sun-photometer, using the calibration curve defined by the best-fit constants R_0 and K determined by Tomasi *et al.* [11].

We then plotted the measurements of ratio R given by each sun-photometer as a function of the square root of ratio $(m_{\mathrm{w}} w p_0/1013.25)$, where w was estimated following the above averaging procedures, and then determined the regression lines in the form of eq. (1), obtaining the empirical values of R_0 and K given in table II. The scatter diagrams and the corresponding regression lines obtained for the six Volz sun-photometers are shown in fig. 4. The entire set of field calibration measurements of R can be seen to follow very closely the square root dependence law of water vapour absorption on the water vapour mass present along the sun-path, the better performances being found for sun-photometers # 595 and 596, the worse one for sun-photometer # 477. Taking into account that the scatter of data is very limited in all cases, we can reasonably state that all the estimates of w obtained through the two procedures are more precise than those

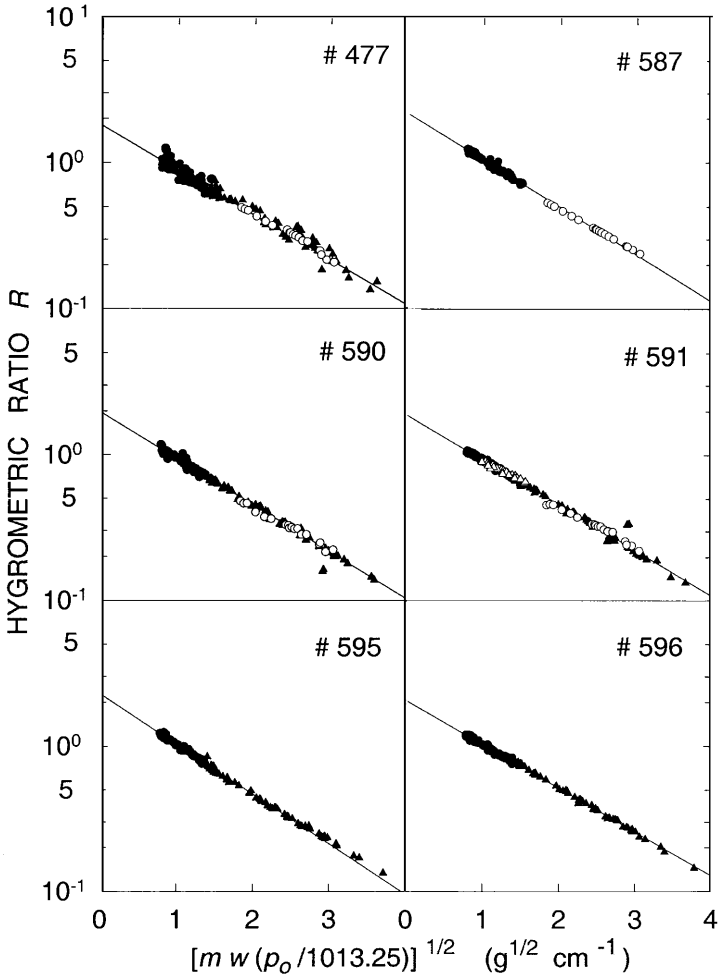

Fig. 4. – Scatter diagrams of the natural logarithms of hygrometric ratio R plotted *vs.* the square root of $m\,w\,(p_0/1013.25)$ as obtained from the calibration measurements performed with the six Volz (model A) sun-photometers at Bologna (solid circles), Molinella (solid triangles), Poggioraso (open circles) and Passo delle Radici (open triangles). The best-fit values of the calibration constants defining the six regression lines are given in table II, together with the corresponding values of the regression coefficient.

provided by the original calibration constants. Thus, the calibration constants given in table II should yield reliable and more homogeneous measurements of w at all mountain stations.

Putting in eq. (2) the new values of the calibration constants proposed in table II, we determined the values of w from the measurements of ratio R calculated from the output voltages given by the Volz sun-photometers. The time-patterns of w defined using the new calibration constants are shown in the right part of fig. 3 for comparison with those previously presented in the left part of fig. 3, as found using the manufacturer's values of R_0 and K. The new time-patterns of w turn out to be considerably less scattered than

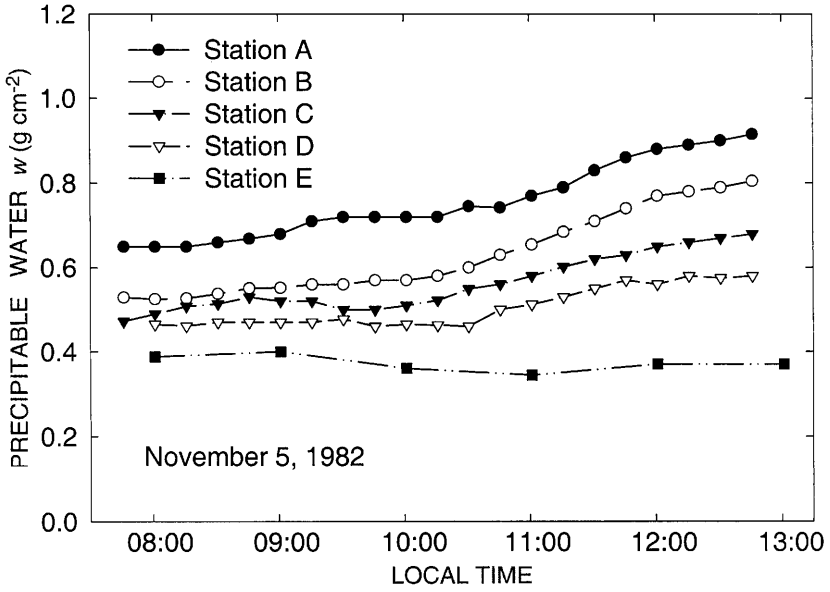

Fig. 5. – Time-patterns of precipitable water w obtained from the simultaneous measurements of hygrometric ratio R carried out on November 5, 1982, with four Volz sun-photometers and the FISBAT sun-photometer (example E) at the five stations listed in table I.

the previous ones: they exhibit discrepancies of no more than 8%, and are considerably smaller than those found using the original values of the calibration constants, which exceeded 35% in the worse cases. The comparison in fig. 3 also confirms that the use of the new calibration constants R_0 and K in eq. (2) enabled us to obtain a more homogeneous set of precipitable water values at all the mountain stations.

4. – Determination of precipitable water time-patterns

The new calibration constants given in table II were used to calculate precipitable water from all the Volz sun-photometer measurements carried out during the two field campaigns, obtaining very homogeneous estimates of w at the four lower stations, as shown in the example of fig. 5, which shows the precipitable water time-patterns measured on November 5, 1982. The values of w at the four lower stations appear in general to appreciably increase throughout the morning, the average trends with slopes decreasing with altitude. The variations are plausibly due not only to the transport of more humid air masses from the bottom of the lower part of the valley toward the upper part and along the valley slopes, as a result of more intense upslope winds, but also to evaporation processes caused by solar radiation at the surface.

Small discrepancies were found between the values of the calibration constants R_0 and K determined for the FISBAT (example E) sun-photometer analysing the measurements carried out in 1981 at the Passo delle Radici station [11] and those obtained from the measurements taken in November 1982, examined through the above intercomparison with the simultaneous measurements taken with the Volz sun-photometer measurements. Thus, we decided to use directly the original calibration constants R_0 and K [11] to

analyse the measurements performed at Mt. Cimone in autumn 1982. The time-patterns of w determined at this high-altitude station were found to be fully consistent with the other results. Those obtained on November 5, 1982, are also shown in fig. 5 to point out that precipitable water remained almost stable in time throughout the morning, showing that the vertical transport effects did not involve the top-level station on that day.

Since hygrometric ratio measurements were not taken during the 1981 campaign at the Mt. Cimone station, where an AM sun-photometer [10] was used, the values of w at this mountain station were calculated taking into account the precipitable water measurements carried out at stations A, B, C and D and the meteorological data routinely recorded by the thermohygrograph placed at the Mt. Cimone (2165 m a.m.s.l.). For this purpose, we first calculated the mean values of absolute humidity within the three layers defined by the A, B, C and D station levels, as found by dividing the differences between the measurements of w found at two nearby stations by the corresponding layer depth values. We assumed that absolute humidity decreases exponentially as a function of height, in the form proposed by Tomasi [34], and then calculated the average values of the scale height by following the procedure described by Tomasi and Paccagnella [35] and using at each measurement-time the mean values of absolute humidity determined within the three atmospheric layers. The average scale height value obtained at a certain measurement-time was then assumed to give form to the vertical profile of absolute humidity from the D station level up to the 1850 m height, which corresponds to the average altitude of the Apennine ridge in the Leo Valley area. Bearing in mind that irregular changes in the absolute humidity features frequently occur in proximity of the Mt. Cimone summit, due to local orographic effects, we separately considered the absolute humidity values simultaneously measured at the top-level station E and assumed that absolute humidity varies linearly with height, passing from the extrapolated value obtained at the 1850 m altitude to that measured at station E. For these assumptions, we calculated the water vapour mass vertical content Δw of the atmospheric layer between the D and E station levels and determined each value of precipitable water at the Mt. Cimone station, by subtracting the mass content Δw from the value of w measured at the station D with the Volz sun-photometer. Figure 6 provides an example of time-patterns of w directly found at the four lower stations from the Volz sun-photometer measurements and evaluated at the highest station by following the above procedure. Precipitable water was found to decrease slowly at the four lower stations and to increase appreciably at Mt. Cimone during the first two measurement hours, suggesting that the extended convective transport occurring on that morning was capable of causing an increase in precipitable water also at the top-level station, while absolute humidity decreased slowly in the subsequent hours.

5. – Vertical profiles of absolute humidity

The results shown in figs. 5 and 6 clearly indicate that precipitable water varies considerably during the morning at all the mountain stations located along the slope of the Leo Valley. Since this phenomenon should be also accompanied by important time-changes in the humidity conditions of the ground layer, we analysed the precipitable water measurements obtained in the previous section to determine the mean values of absolute humidity within the various atmospheric layers defined by the sun-photometer station levels. For this purpose, we first calculated the partial contents Δw of precipitable water within the four layers as differences between the values of precipitable water measured at the lower and upper station level of each layer. We then divided each partial content Δw by the

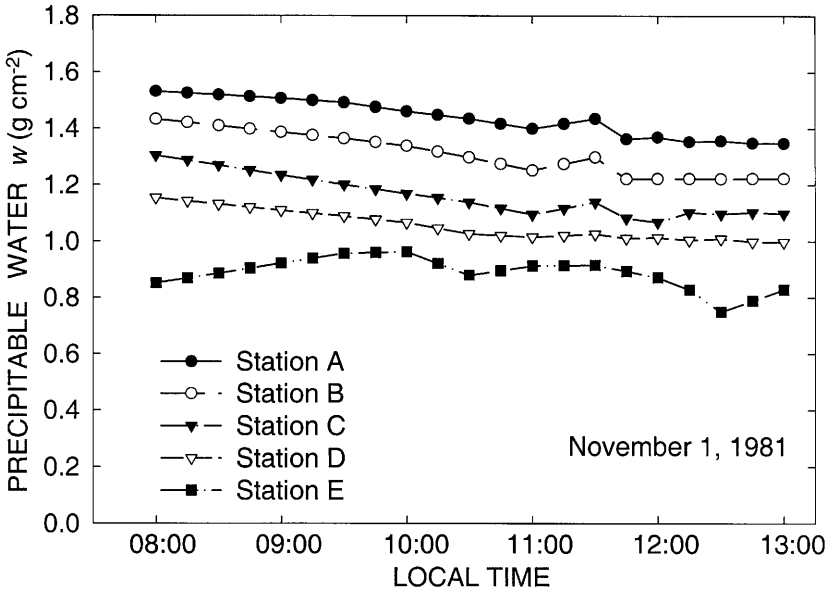

Fig. 6. – As in fig. 5 for the field measurements carried out on November 1, 1981.

corresponding difference Δz between the two station altitudes, obtaining mean evaluations of absolute humidity within the four interposed layers of the atmosphere. Because these estimates were obtained from data on atmospheric vertical columns above different sites and placed at different heights along the valley slope, the vertical profiles of the absolute humidity values cannot be considered as realistic representations of the vertical distribution of this meteorological quantity in the free atmospheric region occupying the central part of the valley section. They can be more correctly regarded as estimates of variations in the ground layer conditions of absolute humidity occurring along the slope of the valley. Two sets of vertical profiles of absolute humidity determined following the above procedure are shown in fig. 7 for the two days presented in figs. 5 and 6, together with the corresponding values of absolute humidity measured at the highest station of Mt. Cimone. Absolute humidity presented very stable values at 08:00 LT of November 1, 1981, within all the four interposed layers, these values being very close to that measured at Mt. Cimone. During the following three hours of the morning, the mean absolute humidity values found within the two lower layers increased markedly, those in the two upper layers diminished considerably, while that of Mt. Cimone remained almost constant in time. From 11:00 LT to 13:00 LT, opposite trends were observed in the various layers, with a marked decrease in the two lower layers and a considerable increase in the upper ones. Such features suggest that the transport of humid air from the lower part of the valley was so intense during the early morning as to modify appreciably the humidity conditions at altitudes lower than 1 km, the subsequent variations being plausibly caused by combined effects due to both transport and evaporation. The vertical profiles of absolute humidity determined on November 1, 1982, exhibit more limited time-variations, characterised by opposite trends to those observed at the various hours in the first layer of the previous example, while similar variations were measured within the other three upper layers, although they were less marked than those of the first example. It is in-

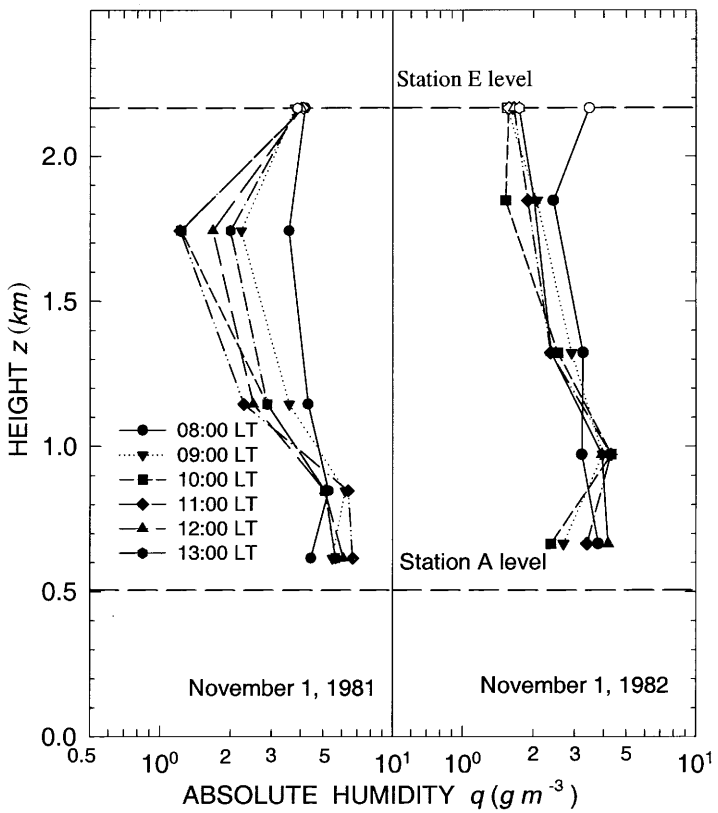

Fig. 7. – Vertical profiles of absolute humidity q determined at six hours on November 1, 1981 (left) and November 1, 1982 (right). The horizontal dashed lines indicate the levels of the two extreme stations A and E, while the open symbols give the values of q simultaneously measured at the meteorological station of Mt. Cimone (2165 m a.m.s.l.).

teresting to notice that the absolute humidity measurements taken at the Mt. Cimone station shows a trend of the same sign as those simultaneously determined within the two upper layers during the whole morning.

It is also important to point out that the absolute humidity time-variations described in fig. 7 indicate that this physical quantity can more than double during the morning at the various heights. Considering that water vapour can cause important absorption effects on the incoming solar radiation, as shown in the Introduction, the time-variations in precipitable water and absolute humidity determined above are expected to produce marked effects on the solar radiation terms of the radiative budget at the ground and at the top-level of the atmosphere.

6. – Evaluations of the water vapour absorption effects on the solar radiation fluxes

To give an idea of the important effects on the incoming solar radiation caused by the attenuation processes generated by the various atmospheric constituents, fig. 8(a) shows the spectral curves of total atmospheric transmittance $\tau(\lambda)$ in the 0.2–2.7 μm wavelength

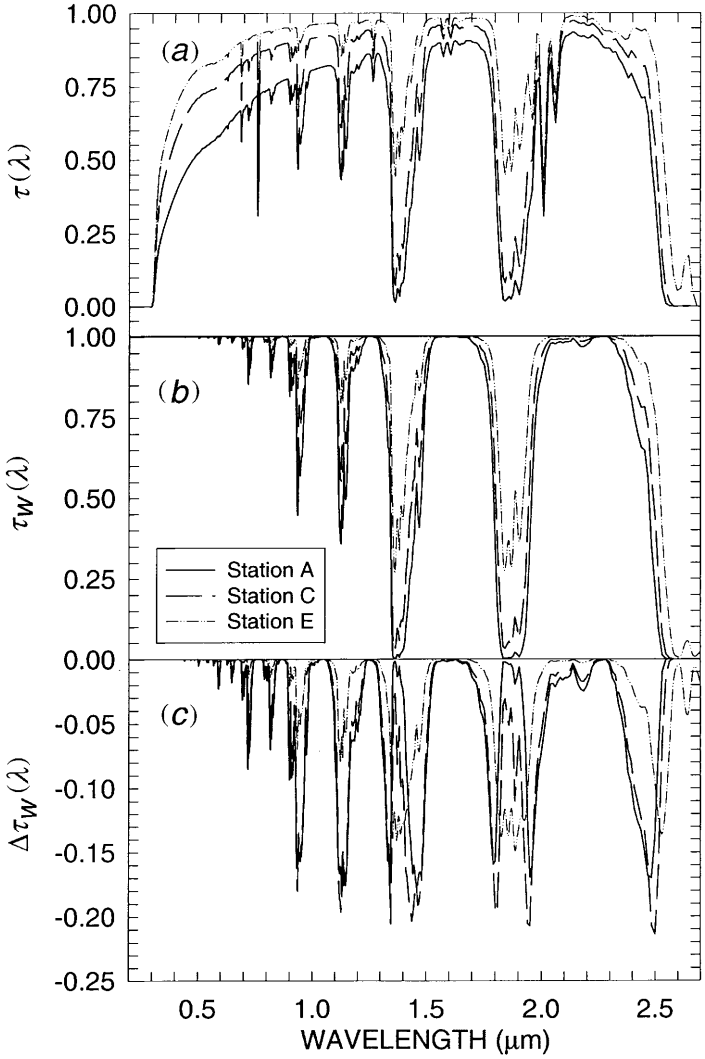

Fig. 8. – (a) Comparison between the spectral curves of total atmospheric transmittance $\tau(\lambda)$ within the 0.2–2.7 μm wavelength range, as calculated along the vertical atmospheric path at the three mountain stations A, C and E for a spectral resolution of 10 nm at wavelength $\lambda = 2$ μm. The calculations were made using the MODTRAN 3.7 code [31] for the atmospheric transparency conditions, precipitable water and rural aerosol optical depth values measured at the 08:30 LT of November 1, 1982 [37]. (b) Spectral curves of partial transmittance $\tau_{\mathrm{w}}(\lambda)$ due to water vapour, calculated at the same three stations along the sun-paths defined at the 12:30 LT of the same day. (c) Spectral curves of the differences $\Delta\tau_{\mathrm{w}}(\lambda)$ between the pairs of spectral curves $\tau_{\mathrm{w}}(\lambda)$ measured at the same three stations at 08:30 and 12:30 LT of November 1, 1982.

range, calculated along the vertical path of the atmosphere using the MODTRAN 3.7 computer code [31] for the atmospheric transmission conditions observed at stations A, C and E on November 1, 1982 (08:30 LT). In these calculations

i) Rayleigh scattering optical depth was evaluated according to the calculations made for the 1962 U. S. Standard Model of the atmosphere [36], taking into account the ground-level pressure values measured at the three stations on that day.

ii) Optical depths due to ozone, nitrogen dioxide, oxygen, sulphur dioxide and many other minor gases were calculated using the MODTRAN 3.7 code [31] for the "U. S. Standard Atmosphere, 1976" [3].

iii) Water vapour optical depth was determined for the precipitable water values measured above at the three stations.

iv) Aerosol optical depth was evaluated throughout the overall spectral range by assuming a) that the aerosol optical depth values at wavelength $\lambda = 550$ nm are equal to those measured at the three stations by Marani *et al.* [37] on the same measurement day, and b) the spectral features of aerosol extinction are those produced by the bimodal size-distribution curve and the radiative properties defined by the rural aerosol model described in the MODTRAN 3.7 code [31].

The spectral curves in fig. 8(a) indicate that atmospheric transmittance varies greatly at visible and near-infrared wavelengths from one station to another, mainly as a result of the variable spectral features of Rayleigh scattering and water vapour absorption. In particular, the absorption effects caused by atmospheric water vapour produce considerable changes in the four spectral intervals covered by the absorption bands Φ, Ψ, Ω and X within the 1–2.7 μm wavelength range [9].

In order to show how intense the effects caused by water vapour can be, we also calculated the spectral curves of the partial transmittance $\tau_{\mathrm{w}}(\lambda)$ relative to the atmospheric water vapour by applying the above calculation procedure to the atmospheric oblique trajectories described by the direct solar radiation beam passing through the atmosphere. Figure 8(b) shows the curves of $\tau_{\mathrm{w}}(\lambda)$ obtained at stations A, C and E at the 12:30 LT of November 1, 1982. As can be seen, differences of more than 10% were often found from one station to another within the spectral intervals containing the four above-mentioned water vapour bands. Thus, considering the pairs of spectral curves of $\tau_{\mathrm{w}}(\lambda)$ determined at 08:30 and 12:30 LT of November 1, 1982, along the sun-paths relative to stations A, C and E, we calculated the differences $\Delta\tau_{\mathrm{w}}(\lambda)$ between them. The results are given in fig. 8(c), indicating that partial transmittance $\tau_{\mathrm{w}}(\lambda)$ was subject to a considerable decrease, by percentages ranging between a few percents and more than 15% from 08:30 LT to 12:30 LT. Such behaviour is to be attributed to the appreciable time-increases in precipitable water observed at the three stations (see fig. 5), as well as the gradual variations with time of the relative optical air mass for water vapour. Figure 8(b) also shows that the most significant decreases in $\tau_{\mathrm{w}}(\lambda)$ take place within the wavelength intervals containing the wings of the four above-mentioned water vapour bands.

The present calculations suggest that the atmospheric transmittance features associated with the time-changes in precipitable water observed at the five Leo Valley stations can cause important changes in the instantaneous downwelling flux Φ_1 of global solar radiation reaching the ground, since both direct and diffuse components of solar radiation turn out to be considerably absorbed by atmospheric water vapour, especially at infrared wavelengths. Thus, we calculated the incoming global flux Φ_1 at various hours of the measurement days by employing the 6S computer code [2], and assuming that

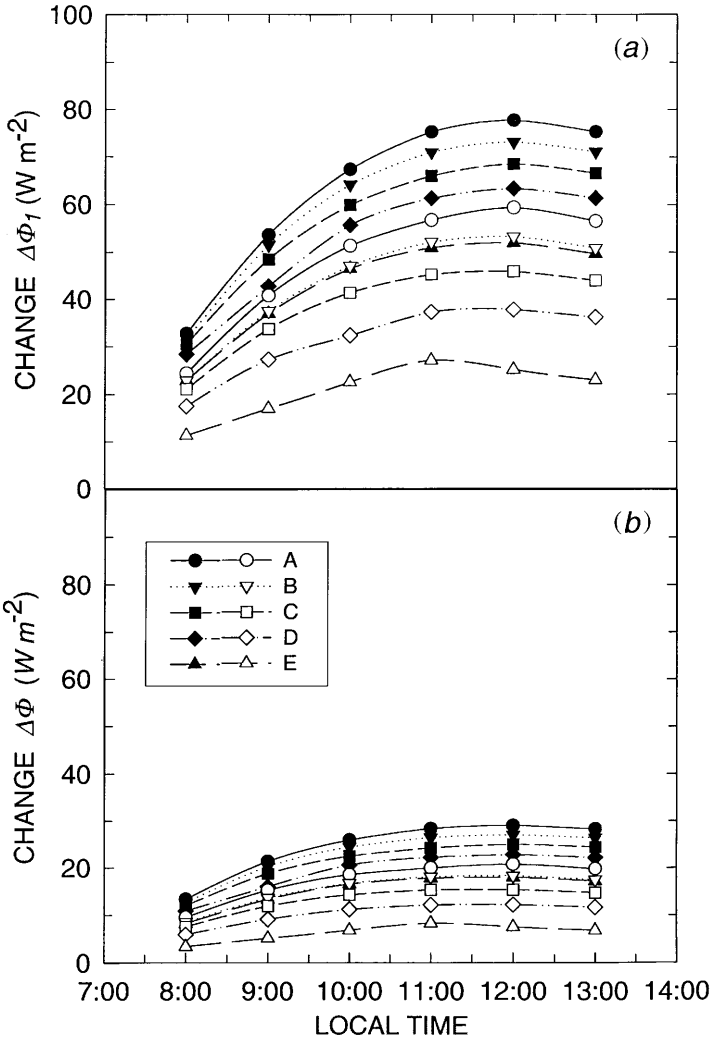

Fig. 9. – (a) Time-patterns of the instantaneous change $\Delta\Phi_1$ produced by water vapour absorption in the downwelling flux Φ_1 of global solar radiation reaching the ground, as calculated at the five mountain stations on November 1, 1981 (solid symbols) and November 1, 1982 (open symbols). (b) Time-patterns of the instantaneous radiative flux change $\Delta\Phi$ caused by water vapour absorption in the upwelling flux Φ of global solar radiation reaching the top-level of the atmosphere, as calculated at the five mountain stations on November 1, 1981 (solid symbols) and November 1, 1982 (open symbols), by assuming that the spectral curve of surface albedo is the same at all the stations, as defined by the 6S computer code [2] for a green vegetation cover.

the spectral extinction characteristics of the atmosphere were those observed during the measurement periods. They were calculated following the procedure adopted above to calculate the time-patterns of atmospheric transmittance $\tau(\lambda)$ in fig. 8(a), where the partial optical depths due to Rayleigh scattering, water vapour and ozone absorption and aerosol extinction were determined on the basis of local measurements of air pressure,

precipitable water and aerosol optical depth at $\lambda = 550$ nm wavelength [37]. The instantaneous incoming flux Φ_1 of global solar radiation was first calculated at all stations for the precipitable water values measured at the various hours of each day, and then by assuming that precipitable water is null. The difference $\Delta\Phi_1$ between each pair of these values of Φ_1 provides the realistic estimate of the change produced by the water vapour absorption in the instantaneous solar radiation flux at ground level. Figure 9(a) shows the time-patterns of $\Delta\Phi_1$ obtained from the precipitable water measurements carried out on November 1, 1981 and 1982. The results indicate that change $\Delta\Phi_1$ gradually increased during the early hours of the morning on both days, reaching the highest values towards noon. The increase of $\Delta\Phi_1$ during the morning is characterised by similar trends at all stations on both days, indicating that the time-variations in the solar elevation angle exert the strongest influence on the incoming flux of global solar radiation, the time-changes in the atmospheric extinction features causing less marked effects. Change $\Delta\Phi_1$ did not exceed 50 and 30 W m^{-2} at the highest station of Mt. Cimone on the two measurement days, respectively, and assumed gradually higher values at the other lower stations, reaching noon-values of nearly 80 W m^{-2} at station A on November 1, 1981, and of about 60 W m^{-2} on November 1, 1982.

The incoming global flux Φ_1 at the ground level is in part absorbed by the terrain and in part reflected backward, to re-cross the atmosphere until reaching outer space. During the second passage through the atmosphere, a certain fraction of solar radiation is involved in Rayleigh scattering, aerosol extinction and water vapour absorption processes. In areas mostly covered by grasslands and forests, like that of the Leo Valley, the surface reflectance presents very low values, ranging mainly between 0.02 and 0.10 at wavelengths from 0.3 to 0.7 μm, and values mostly higher than 0.30 at the near-infrared wavelengths. Thus, only a limited part of flux Φ_1 reaching the ground is reflected upward by the green vegetation cover and subsequently absorbed by water vapour during the passage from the ground level to the top of the atmosphere. Therefore, both the instantaneous upwelling flux Φ of solar radiation leaving the atmosphere and its change $\Delta\Phi$ due to water vapour absorption is expected to be considerably lower than the corresponding quantities Φ_1 and $\Delta\Phi_1$ measured at the ground.

Expectations are confirmed by the calculations of Φ and $\Delta\Phi$ performed by us with the 6S computer code [2]. The instantaneous outgoing flux Φ of global solar radiation was computed at the solar elevation angles for the various hours of the field measurement days by i) determining at regularly-spaced azimuth and zenith angles of the Sun the contributions provided by the direct and diffuse solar radiation components reflected backward by the terrestrial surface, as well as those given by the solar radiation component scattered upward by the atmosphere during its two passages through the atmosphere, and ii) integrating the sum of all these components over the 2π solid angle.

For the calculations, we followed the procedure adopted by Vitale *et al.* [38]. Calculations of flux Φ were carried out for each solar zenith angle, assuming the same spectral extinction characteristics of the atmosphere observed during the measurement days [37] and defined above in the calculations of Φ_1, taking into account the effects due to Rayleigh scattering, aerosol extinction and absorption by water vapour, ozone and other minor gases. The flux Φ was then calculated for the same solar coordinates and atmospheric extinction features but without water vapour. The difference $\Delta\Phi$ between each pair of values of Φ obtained for the same atmospheric model with and without water vapour was considered to be a realistic evaluation of the change caused by water vapour absorption in the outgoing flux Φ.

The results obtained on the same two measurements days considered in fig. 9(a) are

shown in fig. 9(b) for comparison. Mainly as a result of the strong decrease produced by the relatively low surface reflectance characteristics, the change $\Delta\Phi$ assumes on the two days values not higher than 10 and 15 W m^{-2}, respectively, at the Mt. Cimone station, and values lower than 30 W m^{-2} on November 1, 1981, and lower than 20 W m^{-2} on November 1, 1982, at the lowest station situated on the bottom of the Leo valley. Also in these cases, the gradual increase of $\Delta\Phi$ observed at all the stations is clearly governed by the increase of the solar elevation angle, causing the gradual decrease in the relative optical air mass and, hence, in the relative length of the sun-path.

7. – Conclusions

Figure 9 clearly shows that the terms $\Delta\Phi_1$ and $\Delta\Phi$ are strongly influenced by diurnal variations in the relative optical air mass, since this quantity varies considerably during the morning as a function of the solar zenith angle, being with good approximation equal to the secant of the apparent zenith angle of the Sun [4]. The second parameter on which both terms $\Delta\Phi_1$ and $\Delta\Phi$ closely depend is precipitable water. In fact, the global solar radiation flux Φ_1 reaching the ground is strongly absorbed by the water vapour mass along the sun-path, which is approximately given by the product of precipitable water by the relative optical air mass. In reality, the absorption of direct solar radiation varies greatly as a function of the water vapour mass distributed along the sun-path, through a non-linear dependence function closely related to the strong absorption regime regulating the overall absorption of the main water vapour bands in the short-wave spectrum [9]. Thus, the higher is the water vapour mass along the sun-path, the more intense is the absorption strength of the direct and global solar radiation reaching the ground. Consequently, the percentage of global solar radiation measured at the terrestrial surface is expected to considerably diminish during periods when precipitable water and/or relative optical air mass tend to increase with trends similar to those measured during our two campaigns.

Similarly, the change $\Delta\Phi$ in the instantaneous outgoing flux of global solar radiation at the top of the atmosphere is forced to increase as the relative optical air mass decreases throughout the morning, as clearly demonstrated by the results shown in fig. 9(b). The same results also indicate that the change $\Delta\Phi$ undergoes an increase, passing from the higher to the lower stations, as a consequence of the increase in precipitable water. Thus, it can be reasonably stated that change $\Delta\Phi$ varies significantly as a function of the water vapour mass present along the sun-path, since it includes both the water vapour absorption effects on the incoming solar radiation and those directly produced by water vapour on the fraction of solar radiation reflected upward by the surface, and subsequently passing again through the atmosphere, before leaving our planet. The evaluations of $\Delta\Phi$ presented in fig. 9(b) were made at various times of the two days for values of the relative optical air mass decreasing from 6.3 at 08:00 LT to about 2.3 at 10:00 LT, and ranging between 1.9 and 2.0 from 11:00 LT to 13:00 LT. In order to provide evidence of the dependence features of the instantaneous change $\Delta\Phi$ on precipitable water (independently of the time-variations in the relative optical air mass), we have plotted in fig. 10 the values of $\Delta\Phi$ as a function of precipitable water, at 11:00, 12:00 and 13:00 LT of the various measurement days and, hence, calculated for relative optical air masses ranging between 1.9 and 2.0. The results in fig. 10 indicate that the instantaneous change $\Delta\Phi$ increases appreciably from less than 7 W m^{-2} to about 30 W m^{-2} as precipitable water increases from 0.1 to nearly 1.7 g cm^{-2}. Considering that the relative optical air mass is in practice constant for all the evaluations of $\Delta\Phi$, we can assume that the

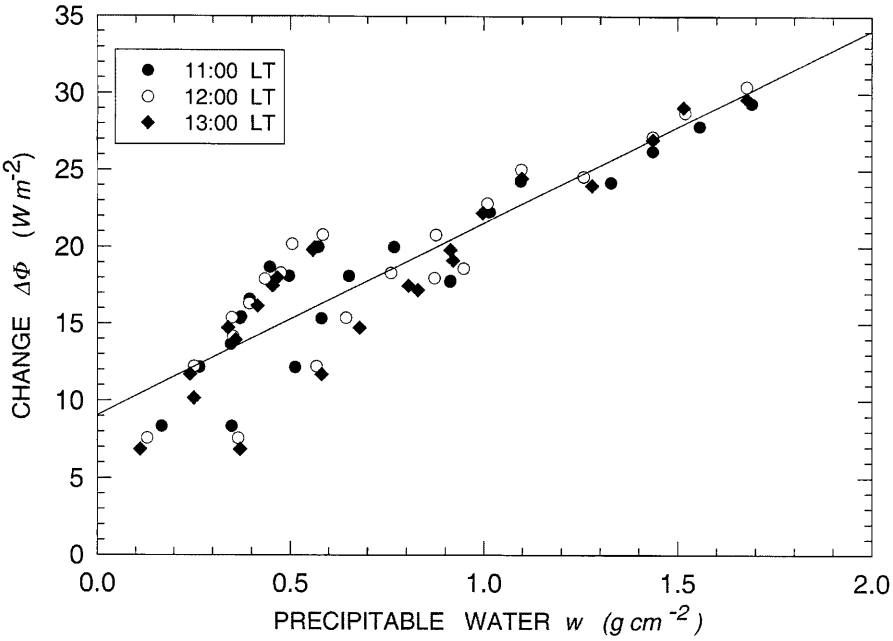

Fig. 10. – Evaluations of the instantaneous radiative flux change $\Delta\Phi$ plotted as a function of precipitable water w, as calculated on six measurement days at 11:00 LT (solid circles), 12:00 LT (open circles) and 13:00 LT (solid diamonds), when the relative optical air mass varies only between 1.9 and 2.0, the solar zenith angle being quite stable during the middle part of the day. The values of $\Delta\Phi$ turn out to be best-fitted by a line found with a regression coefficient of +0.81 and having intercept equal to about 9 W m^{-2} and slope coefficient equal to 12.5 W m^{-2} per unit variation of precipitable water measured in g cm^{-2}.

geometrical configuration of the radiative transfer simulation is in practice the same for all these cases. The best-fit line drawn for these data turns out to have intercept equal to about 9 W m^{-2} and slope coefficient equal to about 12.5 W m^{-2} per unit variation of precipitable water, suggesting that the change $\Delta\Phi$ tends to increase on average by more than 10 W m^{-2} when precipitable water increases by 1 g cm^{-2} during the middle part of the day. In reality, the best-fit line in fig. 10 represents only a rough method for evaluating $\Delta\Phi$, since the relationship suggested by the theory should be more correctly represented by an exponential curve, which is shaped by the atmospheric transmittance rules. Therefore, this relationship curve should be defined by 1) intercept equal to zero in the hypothetical atmosphere, without water vapour and in the absence of indirect interferences caused by aerosols and the other atmospheric constituents in the radiative transfer processes, and 2) a shape whose variability is driven by the dependence features of the strong water vapour bands on the water vapour amount. A theoretical curve should rapidly increase through the range of precipitable water < 1.0 g cm^{-2} and then asymptotically tend to the best-fit line defined in fig. 10 for high values of precipitable water. Moreover, it is important to take into account that aerosol optical depth in general increases with precipitable water, because the increase is generally associated with increasing relative humidity of the air within the lower part of the troposphere, these moisture conditions favouring the growth of aerosol particles and the increase in the

particulate extinction effects, as clearly demonstrated by both field measurements [39] and tropospheric aerosol extinction models determined for different relative humidity conditions of the surrounding air [40]. In the presence of an appreciable increase in the aerosol optical depth at both visible and near-infrared wavelengths, a considerably greater percentage of solar radiation is expected to be involved in scattering processes and, hence, backscattered upwards. Thus, less radiation should be available for water vapour absorption and this could contribute to causing a gradual decrease in $\Delta\Phi$, which becomes gradually more marked as precipitable water increases. This could be a reliable explanation for the fact that the intercept value of the best-fit line defined in fig. 10 was found to be very far from the null value suggested by the theory. The most plausible explanation for the results obtained in fig. 10, showing a non-linear dependence of $\Delta\Phi$ on precipitable water in the lower range of this quantity, is that the intensity of water vapour absorptance within the numerous and extended infrared spectral intervals shown in fig. 8 varies in reality as a power of the water vapour mass in the atmosphere. Thus, corresponding to the variations in the atmospheric water vapour mass along the sun-path, the exponent varies from 1 to 0.5 as the absorption regime of the water vapour bands gradually becomes stronger, passing from the ideal linear law (very weak absorption) to the square-root law (strong absorption) and, hence, following evolutionary patterns similar to those described by the Matheson diagram [41].

REFERENCES

[1] Atkinson B. W., *Mesoscale Atmospheric Circulations* (Academic Press., London) 1981, p. 215.

[2] Vermote E., Tanre' D., Deuze' J. L., Herman M. and Morcrette J. J., *Second Simulation of the Satellite Signal in the Solar Spectrum (6S)*, 6S User Guide Version 2 (Lille, Universitè de Lille, France) 1997.

[3] Anderson G. P., Clough S. A., Kneizys F. X., Chetwynd J. H. and Shettle E. P., *AFGL Atmospheric Constituent Profiles (0 - 120 km)*, Environ. Res. Papers, **No 954**, Air Force Geophysics Laboratory-TR-86-0110 (AFGL, Hanscom L. G. Field, MA) 1986.

[4] Iqbal M., *An Introduction to Solar Radiation* (Academic Press, Toronto) 1983, p. 1.

[5] Russell P. B., Livingston J. M., Hignett P., Kinne S., Wong J., Chien A., Bergstrom R., Durkee P. and Hobbs P. V., *J. Geophys. Res.*, **104** (1999) 2289.

[6] Vitale V., Tomasi C., von Hoyningen-Huene W., Bonafe' U., Marani S., Lupi A., Cacciari A. and Ruggeri P., *Tellus B*, **52** (2000) 716.

[7] Tomasi C., Vitale V. and Marani S., *Vertical distribution curves of aerosol particle extinction from sun-photometer measurements taken at different altitudes in an Apennine valley*, in *IRS '84: Current Problems in Atmospheric Radiation*, edited by G. Fiocco (Deepak A. Publ., Hampton, Virginia) 1984, p. 54.

[8] Volz F. E., *Appl. Opt.*, **13** (1974) 1732.

[9] Kondratyev K. Ya., *Radiation in the Atmosphere* (Academic Press, New York) 1969, p. 85.

[10] WORLD METEOROLOGICAL ORGANIZATION, *Recent Progress in Sunphotometry (Determination of the Aerosol Optical Depth)*, Environmental Pollution Monitoring Research Programme N. 43 (1986).

[11] Tomasi C., Prodi F., Sentimenti M. and Cesari G., *Appl. Opt.*, **22** (1983) 622.

[12] Tomasi C., Vitale V. and De Santis L. V., *Meteorol. Atmos. Phys.*, **65** (1998) 11.

[13] Fowle F. E., *Astrophys. J.*, **35** (1912) 149.

[14] Fowle F. E., *Astrophys. J.*, **42** (1915) 394.

[15] Kimball H. H. and Hand I. F., *Mon. Weather Rev.*, **61** (1933) 80.

[16] Foskett L. W. and Foster N. B., *Bull. Am. Meteorol. Soc.*, **24** (1943) 146.

[17] Gates D. M., *J. Meteorol.*, **13** (1956) 369.
[18] Foster N. B., Volz D. T. and Foskett L. W., *A spectral hygrometer for measuring total precipitable water*, in *Humidity and Moisture, Volume 1: Principles and Methods of Measuring Humidity in Gases*, edited by R. E. Ruskin (Reinhold Publ. Corp., New York) 1964, p. 455.
[19] Goody R. M., *Q. J. R. Meteorol. Soc.*, **78** (1952) 165.
[20] Gates D. M. and Harrop W. J., *Appl. Opt.*, **2** (1963) 887.
[21] Guzzi R., Tomasi C. and Vittori O., *J. Atmos. Sci.*, **29** (1972) 517.
[22] Tomasi C. and Guzzi R., *J. Phys. E*, **7** (1974) 647.
[23] Pitts D. E., McAllum W. E., Heidt M., Jeske K., Lee J. T., Demonbrun D., Morgan A. and Potter J., *J. Appl. Meteorol.*, **16** (1977) 1312.
[24] Bartels R. A., *J. Climate Appl. Meteorol.*, **25** (1986) 1788.
[25] Tomasi C., Vitale V., Tagliazucca M. and Gasperoni L., *SIF Conference Proceedings*, **27** (1990) 187.
[26] Thome K. J., Herman B. M. and Reagan J. A., *J. Appl. Meteorol.*, **31** (1992)157.
[27] Thome K. J., Smith M. W., Palmer J. M. and Reagan J. A., *Appl. Opt.*, **33** (1994) 5811.
[28] Tomasi C., Marani S., Vitale V., Wagner F., Cacciari A. and Lupi A., *Tellus B*, **52** (2000) 734.
[29] Kasten F., *Arch. Met. Geophys. Biokl. Ser. B*, **14** (1966) 206.
[30] Bucholtz A., *Appl. Opt.*, **34** (1995) 2765.
[31] Shettle E. P. and Fenn R. W., *Models for the aerosols of the lower atmosphere and the effects of humidity variations on their optical properties*, Environ. Res. Papers, **No. 676**, Air Force Geophysics Laboratory-TR-79-0214 (AFGL, Bedford, MA.), 1979.
[32] Kneizys F. X., Abreu L. W., Anderson G. P., Chetwynd J. H., Shettle E. P., Berk A., Bernstein L. S., Robertson D. C., Acharya P., Rothman L. S., Selby J. E. A., Gallery W. O. and Clough S. A., *The MODTRAN 2/3 Report and LOWTRAN 7 MODEL*, edited by L. W. Abreu and G. P. Anderson, Contract F19628-91-C.0132, Phillips Laboratory, Geophysics Directorate (PL/GPOS, Hanscom AFB, MA), 1996.
[33] Anawalt R. A. and Boksenberg A., *The Astronomical Almanac for the Year 1989* (U. S. Government Printing Office, Washington, D. C.) 1988, p. B60.
[34] Tomasi C., *J. Geophys. Res.*, **89** (1984) 2563.
[35] Tomasi C. and Paccagnella T., *Pageoph.*, **127** (1988), 93.
[36] Bucholtz A., *Appl. Opt.*, **34** (1995), 2765.
[37] Marani S., Tomasi C. and Vitale V., *Atmos. Res.*, **61** (2002) 89.
[38] Vitale V., Tomasi C., Lupi A., Cacciari A. and Marani S., *Atmos. Environm.*, **34** (2000) 5095.
[39] Vittori O., Tomasi C. and Guzzi R., *J. Atmos. Sci.*, **31** (1974) 261.
[40] Hänel G. and Bullrich K., *Beitr. Phys. Atmos.*, **51** (1978) 129.
[41] Goody R. M., *Atmospheric Radiation. I Theoretical Basis* (Clarendon Press, Oxford) 1964, p. 122.